Event Detection in Wireless Sensor Networks in Random Spatial Sensors Deployments

Pengfei Zhang, Ido Nevat, Gareth W. Peters, Gaoxi Xiao, *Member, IEEE*, and Hwee-Pink Tan, *Senior Member, IEEE*

***Abstract*—We develop a new class of event detection algorithms in Wireless Sensor Networks where the sensors are randomly deployed spatially. We formulate the detection problem as a binary hypothesis testing problem and design the optimal decision rules for two scenarios, namely the Poisson Point Process and Binomial Point Process random deployments. To calculate the intractable marginal likelihood density, we develop three types of series expansion methods which are based on an Askey-orthogonal polynomials. In addition, we develop a novel framework to provide guidance on which series expansion is most suitable (i.e., most accurate) to use for different system parameters. Extensive Monte Carlo simulations are carried out to illustrate the benefits of this framework as well as the quality of the series expansion methods, and the impacts that different parameters have on detection performance via the Receiver Operating Curves (ROC).**

***Index Terms*—Binomial point process, event detection, Poisson point process, series expansions, wireless sensor networks.**

I. Introduction

WIRELESS Sensor Networks (WSNs) have attracted considerable attention due to the large number of applications, such as environmental monitoring, weather forecasts [1], [2], surveillance, health care, and home automation [2], [3]. WSN consists of a set of spatially distributed sensors which monitor a spatial physical phenomenon containing some desired attributes (e.g., pressure, temperature, concentrations of substance, sound intensity, radiation levels, pollution concentrations etc.), and regularly communicate their observations to a Gateway (GW) [4]–[6]. The GW collects these observations and fuses them in order to perform various tasks, based on which effective actions can be taken [3]. The tasks GW may perform include event detection [7], [8], field reconstruction [9], [10], outlier detection [11], [12], localization [13], [14] and many more. The detection problem in WSN is to distinguish between two hypothesis, namely, the absence (Null Hypothesis), or presence (Alternative Hypothesis) of a certain event [15]–[17]. The ability of a WSN to make such decisions is crucial for various applications, for example, the detection of the presence or absence of a target in a surveillance system, the detection of chemical, biological or nuclear plumes and many more [18]–[20]. It is therefore imperative for the WSN to be accurate in detecting the event (high detection rate) while maintaining as low as possible false detection (low false alarm).

Previous works on event detection have concentrated on cases where the sensors deployment (i.e., the locations of the sensors) is **deterministic and known to the GW** ([3], [21]–[26] and references within). For example, in [25] the problem of distributed detection was considered, where the sensors transmit their local decisions over perfectly known wireless channels. In [26] the problem of distributed event detection under Byzantine attack was considered. Theoretical performance analysis was derived in [23] for detection fusion under conditionally dependent and independent local decisions. Distributed detection in WSNs over fading channels with multiple receive antennas at the GW was considered in [24]. In contrast, the problem of event detection where the sensors are **randomly deployed in the field** is largely unexplored [27]–[29]. This problem is of great practical interest because in many cases the locations of the sensors are unknown to the GW. Examples include volcanic activity detection [30]–[33] and nuclear facility monitoring [34]–[36]. In both cases, it may be impossible or very costly to place the sensors around the source. Instead, sensors could be dropped or deployed from an airplane in a random manner.

In the wireless communication literature, there has been great interest in random deployments of wireless networks, see for example [37], [38]. These works make use of tools from stochastic geometry to calculate parameters of interest, such as capacity, Signal-to-Noise-Ratio (SNR) of such systems and mainly consider homogeneous deployments for mathematical tractability. In practice however, it is very unlikely that the sensors would be distributed in space in a spatially homogenous way, but instead a non-homogeneous behavior is more likely to occur.

To address these aspects of random inhomogeneous spatial deployment of sensor networks, new models and algorithms for event detection need to be developed. In addition, it is important for network designers to understand how different parameters would affect the performance of the WSN before deployment, (i.e., number of sensors, region of deployment, level of inhomogeneity of the deployment etc.) in order to obtain the optimal detection performance.

Manuscript received August 11, 2014; revised March 23, 2015 and June 15, 2015; accepted June 21, 2015. Date of publication July 01, 2015; date of current version October 07, 2015. The associate editor coordinating the review of this manuscript and approving it for publication was Prof. Y.-W. Peter Hong.

P. Zhang and I. Nevat are with the Sense and Sense-abilities, Institute for Infocomm Research, Singapore 138632, Singapore.

G. W. Peters is with the Department of Statistical Sciences, University College London (UCL), London WC1E 6BT, U.K.

G. Xiao is with the School of Electrical and Electronic Engineering, Nanyang Technological University, Singapore 639798, Singapore.

H.-P. Tan is with the School of Information Systems, Singapore Management University, Singapore 188065, Singapore.

Color versions of one or more of the figures in this paper are available online at http://ieeexplore.ieee.org.

Digital Object Identifier 10.1109/TSP.2015.2452218

At the heart of distance based algorithms in WSN under random spatial deployment lies the understanding of the distance distribution. Such quantities have been derived under spatial deployment such as Poisson Point Process (PPP) and Binomial Point Process (BPP) [39]–[42]. In [39], sensors are uniformly randomly distributed following a BPP. The authors analyzed various properties of such networks including the distance distribution, moments of distance etc. In [40], the authors considered a more general distribution, namely the PPP and provided analysis of the distance distributions for such networks. In [41] the authors discussed the deployment of cognitive cellular wireless networks. In [42] the authors considered distance distributions on mobile wireless networks. It is important to note that these papers have only tackled homogeneous deployments and the practical cases of non-homogeneous deployments have not been addressed.

In this paper, we develop event detection algorithms in WSN for the case where the sensors are randomly distributed in space and their locations are unknown to the GW. When the target (event) is present/active, it emits energy (acoustic or electromagnetic) which is measured by each of the sensors. All the measurements from the sensors are then aggregated to the GW which decides whether the target is present or absent. We assume an energy decay model in which the amount of energy each sensor measures falls off with distance obeying an inverse power-law where the exponent is known as the path loss exponent [38]. In contrast to previous works which assumed that the locations of the sensors are known to the GW [15], [24], [43], we assume a random spatial deployment. To obtain the optimal decision rule, the likelihood ratio test (LRT) for the two hypotheses (event present/ absent) needs to be evaluated. This involves the calculation of the marginal likelihood density under each hypothesis. While deriving the marginal likelihood under the null hypothesis is trivial, the derivation of the marginal likelihood under the alternative hypothesis is not readily obtained in closed-form, since it involves a multi-variate convolution which cannot be solved exactly. As such, we adopt a principled approach to approximate the marginal likelihood under the alternative hypothesis. To do so, we exploit stochastic geometry techniques to model the placement of the sensors [39]. We then approximate the intractable distribution density via series expansions techniques which are based on an Askey-orthogonal polynomial expansion. The three series expansions we develop are the Gram-Charlier, Gamma-Laguerre and Beta-Jacobi series expansions. Since these expansions do not ensure positivity of the density at all points, it is important to characterise the system parameters for which the density approximation will remain positive. This characterisation can be carried out by finding the appropriate regions in the Skew-Kurtosis plane (S-K plane) which generate positive support [44], [45]. This characterisation is important and should be used as a guide to choose the appropriate series expansion. We will illustrate the implications of not choosing the correct series expansion via simulations. Importantly, the algorithms we develop only require deriving the first four cumulants and moments to obtain good detection performance and are therefore of low computational complexity.

We summarize our four key contributions as follows.

1) We extend the distance distribution results of [39], [40] for Poisson Point Process and Binomial Point Process to the inhomogeneous deployment case (presented in Theorem 1). These results are required in order to develop the optimal detection algorithm we derive.
2) We develop three different types of Askey-orthogonal polynomial expansion methods to approximate the marginal likelihood density (presented in Section IV). The first is based on Hermite polynomials and is known as the Gram-Charlier series expansion; the second is based on Laguerre polynomials and is known as the Gamma-Laguerre series expansion; the third expansion that we derive for the first time is the Beta-Jacobi series expansion and is based on Jacobi polynomials (presented in Theorem 2 and Theorem 3).
3) We develop a novel analysis tool to characterise the conditions (Skew-Kurtosis region) at which each expansion has a positive support (presented in Section IV). The new tool is of great importance as it provides a guidance as to which series expansion to use under different type of system parameters, such as noise distribution, path-loss exponent parameter, SNR value etc.
4) We show that our proposed Beta-Jacobi series expansion provides better detection performance than the standard Gram-Charlier Gamma-Laguerre series expansions for different practical scenarios.

II. System Model and Problem Formulation

In this section we present the model assumptions. We begin with a formal definition of the Finite Binomial Point Process and Infinite Poisson Point Process followed by system model assumptions. These processes are special cases of spatial point process. In general a spatial point process is a random pattern of points, in our case in 2-dimensional space.

Definition 1 (Finite Binomial Point Process (FBPP) [46], [47]): A Finite Binomial Point Process is defined by considering a fixed number of n points at random locations in a bounded region $W \subset \mathbb{R}^2$. Define by $X_1, \ldots, X_n$ the i.i.d. random locations with the intensity of the number of points in a small region around any location $\mathbf{x}$ denoted as $\lambda(\mathbf{x})$. This produces a probability density of each X_i given by

$$f_X(x) = \begin{cases} \frac{1}{A(W)}, & \text{if } x \in W, \\ 0, & \text{otherwise,} \end{cases}$$

where $A(W)$ denotes the area of W. Each random point X_i is uniformly distributed in W so that for a bounded set, $B \subset \mathbb{R}^2$ has the distribution

$$\mathbb{P}\mathrm{r}\left(X_i \in B\right) = \int_B f_X(x)dx = \frac{A(B \cap W)}{A(W)}.$$

We consider a general case involving an inhomogeneous version of the finite domain spatial BPP (inhomogeneous FBPP). The distribution of the points will have a density $f_X(x)$ given by the decaying power law, relative to the center of W which is specified to be a disc in our applications. Therefore it will have a form given according to

$$f_X(\mathbf{x}) = \|\mathbf{x}\|^{-\nu} \mathbf{1}_W(\mathbf{x})$$

where $\mathbf{1}_W(\mathbf{x})$ is the indicator function defined as:

$$\mathbf{1}_W(\mathbf{x}) = \begin{cases} 1, & \text{if } x \in W \\ 0, & \text{otherwise,} \end{cases}$$

with reference to the center of W.

The second point process is an Infinite Poisson Point Process (IPPP) defined on an infinite domain according to Definition 2.

Definition 2 (Infinite Poisson Point Process (IPPP) [46]): Consider a locally compact metric space $W \subseteq \mathbb{R}^2$ and measure Γ on W which is finite on every compact set and contains no atoms. Then the spatial PPP on W with intensity measure Γ is a point process on W such that

- *for every compact set $B \subset W$, the count $N(B)$ is distributed according to a Poisson distribution with $\Gamma(B)$ mean; and*
- *if $B_1, \ldots, B_m$ are disjoint compact sets, then $N(B_1), \ldots, N(B_m)$ are independent.*

In the examples considered in this paper we will utilise one of two possibilities:

- Homogeneous IPPP (HIPPP), when λ is constant.
- Non-homogeneous IPPP (NIPPP), when λ is not constant. We consider a power law $\lambda(\mathbf{x}) = \|\mathbf{x}\|^{-\nu}$ with $\nu > 0$. Although we claim that the density is of the power law form, the scheme can handle other density distributions as long as the p in Appendix A, proof of theorem 1 can be solved in analytic form in analytic form and that all the moments can be tractable.

The difference between the FBPP and the IPPP is that the number of points n within set V, is a *known constant* under FBPP, and is a *random unknown* under IPPP. For the PPP deployment, there is no need to assume that the source is in the canter of the region. For the BPP, this assumption is required. In any case, for practical scenarios, it is reasonable to assume that the deployment of the sensors would be around the source, therefore, having the source at the centre of the region.

A. Wireless Sensor Network Operation Model

We now present the system model for the WSN.

1) The source is present ($\mathcal{H}_1$) or absent ($\mathcal{H}_0$). Under $\mathcal{H}_1$, the source transmits at a constant power P_0, and under $\mathcal{H}_0$, the source does not transmit ($P_0 = 0$).
2) The location of the source (if present) is assumed to be known at $\mathbf{x}_s = [x_0, y_0]$. We assume it is located at the center of circle of radius R.
3) Consider a WSN consisting of sensors with locations following either a FBPP deployment (Definition 1) or an IPPP deployment (Definition 2) in a 2 dimensional region.
   a) For the FBPP deployment, N_B sensors are deployed in a circle with radius R.
   b) For the IPPP deployment, an unknown random number of sensors are deployed in a circle with radius R. Note that for the case of IPPP, the number of points N_P is not fixed.

   The spatial density of the sensors is given by $\lambda(\mathbf{x}) = \|\mathbf{x}\|^{-\nu}, \nu \neq 0$, where $\|\mathbf{x}\|$ denotes the norm of $\mathbf{x}$.
4) The unknown random location of the $k-th$ nearest sensor to the source ($k = \{1, \ldots, N_i\}, i = \{B, P\}$) is $\mathbf{x}_k = [X_k, Y_k]$.
5) The amount of energy the k-th sensor measures is inversely proportional to the Euclidean distance between the source and the sensor and is given by $\sqrt{P_0} R_k^{-\alpha/2}$. The random variable R_k represents the random distance between the k-th nearest sensor and the source. This distance is defined as the minimum radius of the ball with center $\mathbf{x}_s$, that contains at least k points in the ball, i.e., $R_k = \inf\{r : \{R_{(1)}, R_{(2)}, \ldots, R_{(k)}\} \in B_{\mathbf{x}_s}(r)\}$. $B_{\mathbf{x}_s}(r)$ is the ball with radius r and center at $\mathbf{x}_s$.
6) We assume that a power control mechanism between the nodes and the GW is implemented. Since the sensors are static, this power control is constant over time, similar to the deployment in [30]. Once this has been achieved, the sensors start to collect and transmit their observations to the GW. The observed signal at the GW in the l-th time slot ($l = \{1, \ldots, L\}$) is a linear combination of all the signals given by:

$$\begin{cases} \mathcal{H}_0 : Y_l = W_l \\ \mathcal{H}_1 : Y_l = \sum\limits_{k=1}^{N_i} \sqrt{P_0} {R_k}^{-\alpha/2} + W_l, \end{cases}$$

   where $i = \{B, P\}\ldots., W_l$ is the i.i.d. additive Gaussian noise $\mathcal{N}(0, \sigma^2_{W_l})$. The parameter α is the path-loss coefficient. We note that our model is general enough to cover the cases where sensors may be faulty or outside the communication range of GW by considering the number of active nodes as a random variable.

We proceed by presenting the optimal decision rule for the event detection. We then derive the various components required in order to evaluate the optimal decision rule.

B. Optimal Event Detection Decision Rule

The optimal decision rule is a threshold test based on the likelihood ratio [48]. We consider a frame-by-frame detection, where the length of each frame is L. The decision rule is then given by:

$$\Lambda\left(Y_{1:L}\right) \triangleq \frac{p(Y_{1:L}|\mathbf{x}_s, \mathcal{H}_0)}{p\left(Y_{1:L}|\mathbf{x}_s, \mathcal{H}_1\right)} \underset{\mathcal{H}_1}{\overset{\mathcal{H}_0}{\gtrless}} \gamma, \tag{1}$$

where the threshold γ can be set to assure a fixed system false-alarm rate under the Neyman-Pearson approach or can be chosen to minimize the overall probability of detection error under the Bayesian approach [49]. We decompose the full marginals under each hypothesis, $p\left(Y_{1:L}|\mathbf{x}_s, \mathcal{H}_k\right)$, $k = 0, 1$:

$$p(Y_{1:L}|\mathbf{x}_s, \mathcal{H}_k) = p(Y_1|\mathbf{x}_s, \mathcal{H}_k) \prod_{l=2}^{L} p(Y_l|Y_{1:l-1}, \mathbf{x}_s, \mathcal{H}_k).$$

Next, we can write the l-th observation recursively as:

$$Y_l = \sum_{i=1}^{l-1} \frac{Y_i}{l-1} - \sum_{i=1}^{l-1} \frac{W_i}{l-1} + W_l,$$

and $p(Y_l|Y_{1:l-1}, \mathbf{x}_s, \mathcal{H}_1) \sim N(\sum_{i=1}^{l-1} \frac{Y_i}{l-1}, \frac{l}{l-1}\sigma^2_W)$.

Under $\mathcal{H}_0$ we have that $p(Y_l|Y_{1:l-1}, \mathbf{x}_s, \mathcal{H}_0) \sim N(0, \sigma^2_W)$.

This decomposition is useful as it allows us to work on a lower dimensional space, resulting in efficiency gains for the algorithm we develop and requiring no memory storage.

III. Event Detection Algorithm Under Random Point Process Sensor Deployment

The optimal decision rule in (1) involves calculating the marginal likelihood under each hypothesis, $p\left(Y_{1:L}|\mathbf{x}_s,\mathcal{H}_k\right)$, $k=0,1$. The marginal likelihood under $\mathcal{H}_0$ follows a Normal distribution. The marginal likelihood under the alternative hypothesis, $p\left(Y_l|\mathbf{x}_s,\mathcal{H}_1\right)$, is not attainable in closed form because it involves solving the (N_i+1)-fold convolution as we will show in this section (see (2)). We will therefore develop a novel approximation of the marginal likelihood under the alternative hypothesis, based on an Askey-orthogonal polynomial expansion. In particular, we will derive the Gram-Charlier, Gamma-Laguerre and Beta-Jacobi series expansions.

We begin by extending the earlier work of [39] to obtain the distribution of the distance between the k-th sensor and the source location, denoted by $f_{R_k}(r|\mathbf{x}_s,\mathcal{H}_1)$ for both BPP and IPPP deployments.

Theorem 1: The density of the Euclidean distance between the k-th sensor and the source, R_k, is given by:

1) *BPP deployment:*

$$f_{R_k}\left(r|\mathbf{x}_s,\mathcal{H}_1\right)=\frac{(2-\nu)\,\Gamma\left(k+\frac{1-\nu}{2-\nu}\right)\Gamma\left(N_B+1\right)}{R\,\Gamma\left(k\right)\Gamma\left(N_B+\frac{1-\nu}{2-\nu}+1\right)}\times\beta\left(\left(\frac{r}{R}\right)^{2-\nu};k+\frac{1-\nu}{2-\nu},N_B-k+1\right).$$

2) *IPPP deployment:*

$$f_{R_k}\left(r|\mathbf{x}_s,\mathcal{H}_1\right)=\frac{(2\pi)^k}{\Gamma\left(k\right)(2-\nu)^{k-1}}r^{(2-\nu)k-1}\exp\left(-\frac{2\pi r^{2-\nu}}{2-\nu}\right),$$

where $\beta\left(x,\alpha,\beta\right):=\frac{1}{B(\alpha,\beta)}x^{\alpha-1}\left(1-x\right)^{\beta-1}$ is the β distribution and $\Gamma\left(n\right):=(n-1)!$ is the Gamma function. For both cases, the support of R_k is $Z_k\in R^+$.

Proof: See Appendix A. □

Corollary 1: When $N_B\to+\infty$ and $R\to+\infty$, the non-homogenous BPP converges to an IPPP. Since $p=(r/R)^{2-\nu}$, then $R=rp^{-\frac{1}{2-\nu}}$. Also, $N_P=\int_W\lambda(r)dr=\frac{2\pi}{2-\nu}R^{2-\nu}$. We have $p=(r/R)^{2-\nu}=\frac{2\pi r^{2-\nu}}{N(2-\nu)}$. The density f_{R_k} is given by:

$$\begin{aligned}
&f_{R_k}\left(r|\mathbf{x}_s,\mathcal{H}_1\right)\\
&=\lim_{N_P\to+\infty}\frac{-\nu+2}{r}\frac{(1-p)^{N_P-k}p^k\Gamma(N_P+1)}{\Gamma(N_P-k+1)\Gamma(k)}\\
&=\frac{(2\pi)^k}{\Gamma(k)(2-\nu)^{k-1}}r^{(2-\nu)k-1}\exp\left(-\frac{2\pi r^{2-\nu}}{2-\nu}\right)\\
&\quad\times\lim_{N_P\to+\infty}\frac{\prod_{i=0}^{k-1}(N_P-i)}{N_P^k}\\
&=\frac{(2\pi)^k}{\Gamma(k)(2-\nu)^{k-1}}r^{(2-\nu)k-1}\exp\left(-\frac{2\pi r^{2-\nu}}{2-\nu}\right)\\
&\quad\times\left(1+\mathcal{O}\left(\frac{N_P^k}{N_P^k}\right)\right)\\
&=\frac{(2\pi)^k}{\Gamma(k)(2-\nu)^{k-1}}r^{(2-\nu)k-1}\exp\left(-\frac{2\pi r^{2-\nu}}{2-\nu}\right).
\end{aligned}$$

Next, based on the result in Theorem 1, we derive the density distribution of each of the elements in the observation under the alternative hypothesis Y_l. This involves the non-linear transformation of the random distance, namely $f_{Z_k}\left(r^{-\alpha/2}|\mathbf{x}_s,\mathcal{H}_1\right)$, where $Z_k=R_k^{-\alpha/2}$.

Lemma 1: The density $f_{Z_k}\left(z|\mathbf{x}_s,\mathcal{H}_1\right)=f_{Z_k}\left(r^{-\alpha/2}|\mathbf{x}_s,\mathcal{H}_1\right)$ is given by:

1) *BPP deployment:*

$$f_{Z_k}\left(z|\mathbf{x}_s,\mathcal{H}_1\right)=\frac{2\left(2-\nu\right)}{\alpha R}\frac{\Gamma\left(k+\frac{1-\nu}{2-\nu}\right)\Gamma\left(N_B+1\right)}{\Gamma\left(k\right)\Gamma\left(N_B+\frac{1-\nu}{2-\nu}+1\right)}\times\beta\left(\left(\frac{z^{-2/\alpha}}{R}\right)^{2-\nu};k+\frac{1-\nu}{2-\nu},N_B-k+1\right)z^{-2/\alpha-1}.$$

2) *IPPP deployment:*

$$f_{Z_k}\left(z|\mathbf{x}_s,\mathcal{H}_1\right)=\frac{(2\pi)^k}{\Gamma\left(k\right)(2-\nu)^{k-1}}\left(\frac{2}{\alpha}\right)\times z^{-2/\alpha((2-\nu)k)-1}\exp\left(-\frac{2\pi}{2-\nu}z^{-2/\alpha(2-\nu)}\right).$$

For both cases, the support of Z_k is $Z_k\in\left(R^{-\alpha/2},\infty\right)$.

Proof: See Appendix B. □

Now that we have derived the density and distribution of each of the elements in Y_l, we need to derive the density of the term $\sum_{k=1}^{N_i}\sqrt{P_0}Z_k$. We express this random sum of Y as an N_i-fold convolution of $Z_k, k\in\{1,\ldots,N_i\}$, given by

$$\begin{aligned}
f_Y(y)=*_{i=1}^{N_i}f_{Z_i}(y)&=\int_{-\infty}^{\infty}f_{Z_1}(y-w_1)\cdots\\
&\quad\times\int_{-\infty}^{\infty}f_{Z_{N_i-1}}(y-w_{N_i})f_{Z_{N_i}}(w_{N_i})dw_{N_i}\cdots dw_1,
\end{aligned}\tag{2}$$

where $*$ represents the convolution operation. Each of these convolution integrals is intractable and cannot be solved analytically in closed form. To approximate the marginal likelihood Y_l we will utilise a series expansion approach presented in the next section.

IV. Probability Density Approximation via Series Expansion Methods

In order to evaluate the marginal likelihood in (2), we derive novel approximation for the marginal likelihood. We develop three different series expansion methods for representing the marginal likelihood using orthogonal basis functions [44], [45]. We will show how these expansions are applicable under different scenarios. The series expansions we utilise are based on a kernel density multiplied by polynomials, known as Askey polynomials [50]. Typical Kernel densities include Gaussian density basis, Gamma density basis and Beta density basis. The respective Askey polynomials [50] are Hermite polynomials, Laguerre polynomials and Jacobi polynomials. These series expansions for the scalar case can be generically expressed as follows:

$$f\left(y\right)=g\left(y\right)\left(1+\sum_{j=1}^{\infty}d_jH_j\left(y\right)\right),\tag{3}$$

where $g(y)$ is the kernel, d_j is the j-th weight and $H_j(y)$ is the j-th order basis function. All of these series expansion methods use the basic properties of orthogonality between density functions and polynomials. This property guarantees the integration of density to be equal to one [44], [45]. Each of these series expansion has different properties and different supports. An important aspect of these expansions (due to limited number of terms, specifically four terms will guarantee good performance) is that they do not ensure positivity of the density at all points (for example, it can be negative for particular choices of Skew and Kurtosis). It is therefore important to characterize these values that produce the "envelope" for the density approximation in which it will remain positive. This characterization can be carried out by finding the appropriate regions in the Skew-Kurtosis plane (S-K plane) which generate positive support [44], [45].

We will derive three series expansion methods, which will be used for different practical scenarios (e.g., different system parameters). The first two are the Gram-Charlier and Gamma-Laguerre series expansions. We then develop a new series expansion which we term the Beta-Jacobi series expansion.

A. Gram-Charlier Series Expansion

The Gram-Charlier series expansion utilizes a Gaussian kernel, $g(y)$, and Hermite polynomials, $H_s(x)$, as basis functions. These polynomials are defined in terms of the derivatives of the normal density, $g(y)$ as follows:

$$\frac{\mathrm{d}^s g(y)}{\mathrm{d}^s y} = (-1)^s H_s(y)\, g(y).$$

The Gram-Charlier series expansion is given by:

$$f_Y(y) = \frac{1}{\sqrt{2\pi}\kappa_2} \exp\left(-\frac{(y-\kappa_1)^2}{2\kappa_2^2}\right) \sum_{r=1}^{\infty} \frac{\kappa_r}{r!} \frac{-\mathrm{d}^r(g(y))}{\mathrm{d}^r y},$$

where $g(y)$ is the normal density and κ_r is the r-th cumulant of Y. If we include only the first two correction terms to the normal distribution, we obtain the *Gram-Charlier A* series presented next.

Lemma 2 (Gram-Charlier a Series Expansion): The fourth order approximation of a probability distribution, $f_Y(y)$, via the Gram-Charlier A series is given by

$$f_Y(y) \approx \frac{1}{\sqrt{2\pi}\kappa_2} \exp\left(-\frac{(y-\kappa_1)^2}{2\kappa_2^2}\right) \times \left(1 + \frac{\kappa_3}{6\kappa_2^3} H_3\left(\frac{y-\kappa_1}{\kappa_2}\right) + \frac{\kappa_4}{24\kappa_2^4} H_4\left(\frac{y-\kappa_1}{\kappa_2}\right)\right), \quad (4)$$

where $H_3(y) = y^3 - 3y$ and $H_4(y) = y^4 - 6y^2 + 3$ are the Hermite polynomials, and $\kappa_1, \kappa_2, \kappa_3, \kappa_4$ are the first, second, third and fourth cumulants of Y.

As mentioned before, it is important to characterise the regions in the S-K plane which yield positive support of the density. This is presented in the following Lemma.

Lemma 3 (Positive Density Conditions [44]) : The Gram-Charlier A series expansion yields positive values for the density $f_Y(y)$ only if:

$$\begin{cases} s(\tilde{y}) = -24\frac{H_3(\tilde{y})}{d(\tilde{y})}, \\ k(\tilde{y}) = 72\frac{H_2(\tilde{y})}{d(\tilde{y})}, \end{cases}$$

where $s(\tilde{y})$, $k(\tilde{y})$ denotes the skewness and kurtosis of random variable $\tilde{y}$, $H_i(\tilde{y})$, $i = 1, 2, 3,4$ refers to the i-th orders of polynomials. Also, $\tilde{Y} = \frac{Y-\kappa_1}{\kappa_2}$ and $d(\tilde{y}) = 4H_3^2(\tilde{y}) - 3H_2(\tilde{y})H_4(\tilde{y})$.

B. Gamma-Laguerre Series Expansion

The Gamma-Laguerre series expansion approximates a probability distribution, $f_Y(y)$, by utilizing the orthogonality between the Gamma density kernel and the Laguerre polynomials in order to obtain an efficient series expansion [45]. In contrast to the Gram-Charlier series expansion where the Hermite polynomials have support on the entire real line, the Laguerre polynomials only have support on the positive real line $y \in \mathbb{R}^+$. Instead of directly working with y, we first rescale it to a R.V. $\widetilde{y}$ by $\widetilde{y} = by$, where $b = \frac{\mathbb{E}[y]}{\mathrm{Var}[y]}$ and set $a = \frac{\mathbb{E}[y]^2}{\mathrm{Var}[y]}$. Denoting the density of $\widetilde{y}$ as $f_{\widetilde{y}}$, we express $f_{\widetilde{y}}$ as follows:

$$f_{\widetilde{y}}(\widetilde{y}) = g(\widetilde{y}; a) \sum_{n=1}^{\infty} A_n L_n^{(a)}(\widetilde{y}),$$

where the kernel is the Gamma density, i.e., $g(\widetilde{y}; a) = \frac{\widetilde{y}^{a-1}\exp^{-\widetilde{y}}}{\Gamma(a)}$, with shape $= a$ and scale $= 1$, and the orthonormal polynomial basis (with respect to this kernel) is given by the Laguerre polynomials (in contrast to Hermite polynomials in the Gaussian case of the Gram-Charlier expansion), defined as

$$L_n^{(\alpha)}(x) = (-1)^n x^{1-a} \exp(-x) \frac{d^n}{dx^n}\left(x^{n+a-1}\exp(-x)\right).$$

Next we characterise the S-K region of the Gamma-Laguerre series expansion in which it yields positive support. These results are based on those derived in [45].

Lemma 4 (Positive Density Conditions): The Gamma-Laguerre series expansion yields positive values for the density $f_X(x)$ if:

$$\begin{cases} s(x) = -\frac{1}{B_1}\left(\mu_4(x)B_2 + B_3\right) \text{ for } x \in [0, +\infty) \\ k(x) = \left(\frac{B_1' B_3}{B_1} - B_3'\right)\left(B_2' - \frac{B_1' B_2}{B_1}\right)^{-1}, , \end{cases}$$

where $s(x)$, $k(x)$ refers to the skewness and kurtosis of the random variable X, B_1, B_2, B_3, B_1', B_2' and B_3' are defined in [45].

C. Beta-Jacobi Series Expansion

In this section we develop a series expansion that is based on the Beta kernel. This new expansion is relevant for cases where Y has a bounded support $[a, b]$. To achieve this, we construct the series based on a Beta kernel (instead of Gamma or Normal kernels as before) and the Jacobi polynomials. It is important to note that the Jacobi polynomials are only orthogonal

on $[-1,1]$. Hence, we need to transform Y so that it also has support $[-1,1]$. This is achieved via the transformation

$$X=\frac{2}{b-a}\left(Y-\frac{a+b}{2}\right).$$

We now present our novel Beta-Jacobi density series expansion, see discussions in [51].

Theorem 2 (Beta-Jacobi Density Series Expansion) : The Beta-Jacobi series expansion is given by:

$$f_X(x)=\frac{(x+1)^{\theta-1}(1-x)^{\eta-1}}{B(\theta,\eta)2^{\theta+\eta-1}}\sum_{i=0}^{d}a_iP_i^{(\eta-1,\theta-1)}(x),$$

where the coefficients, a_i, and the Jacobi polynomials, $P_i^{(\eta-1,\theta-1)}(x)$, are given by:

$$\begin{aligned}a_i=&\sum_{j=0}^{i}\mathbb{E}\left[X^j\right]\frac{B(\theta,\eta)(2i+\theta+\eta-1)\,i!}{\Gamma(i+\theta)}\\&\times\sum_{m=j}^{i}\frac{\Gamma(\eta+\theta+i+m-1)}{\Gamma(i-m+1)\Gamma(\eta+m)\,m!2^m}\binom{m}{j}(-1)^{m-j}\\P_i^{(\eta-1,\theta-1)}(x)=&\frac{\Gamma(\eta+i)}{\Gamma(\eta+\theta+i-1)}\\&\times\sum_{m=0}^{i}\frac{\Gamma(\eta+\theta+i+m-1)}{\Gamma(i-m+1)\Gamma(\eta+m+1)\,m!}\left(\frac{x-1}{2}\right)^m.\end{aligned}$$

Proof: See Appendix C. □

The distribution of Y is obtained from the distribution of X via the transformation

$$f_Y(y)=\frac{2}{b+a}f_X\left(\frac{2(y+a)}{b+a}-1\right),\tag{5}$$

where $f_X(x)$ is given in Theorem 2. The values of θ,η need to be chosen in order to find a good approximation of X. We find approximate values of θ,η through K-S curve as mentioned below. Next we find the Skew-Kurtosis conditions to guarantee positive density:

Theorem 3 (Positive Density Conditions): The Beta-Jacobi series expansion yields positive values for the density $f_X(x)$ if:

$$\begin{cases}s(x)=-\frac{1}{B_1}\left(\mu_4(x)B_2+B_3\right)\text{ for }x\in[-1,+1)\\k(x)=\left(\frac{B_1'B_3}{B_1}-B_3'\right)\left(B_2'-\frac{B_1'B_2}{B_1}\right)^{-1}\end{cases},$$

where $s(x)$, $k(x)$ refers to the skewness and kurtosis of the random variable X, $B_1,B_2,B_3,B_1',B_2',B_3'$ are defined in Appendix D.

Proof: See Appendix D □

Utilizing these three series expansions involves calculating the first four cumulants and moments of the model under IBPP and IPPP, which will be presented in the next section.

V. Calculation of the Moments

To obtain the cumulants we need to calculate the Moment Generating Function (MGF) of $Y_l|\mathcal{H}_1$, given by

$$M_{Y_l|\mathcal{H}_1}(t)=M_{Z_1}(t)M_{Z_2}(t)\cdots M_{Z_{N_i}}(t)M_{W_l}(t).$$

Calculating the MGF of each of the elements, Z_k, as presented in Lemma 1 for BPP and IPPP, involves the following:

1) BPP deployment:

$$\begin{aligned}M_{Z_k}(t)=&\mathbb{E}_{f_{Z_k}}\left[\exp(tz)\right]=\int w(k)z^{-2/\alpha-1}\exp(tz)\\&\times\beta\left(\left(\frac{z^{-2/\alpha}}{R}\right)^{2-\nu};k+\frac{-\nu}{1-\nu},N_B-k+1\right)\mathrm{d}z,\end{aligned}$$

where

$$w(k)=\frac{2(2-\nu)}{\alpha R}\frac{\Gamma\left(k+\frac{1-\nu}{2-\nu}\right)\Gamma(N_B+1)}{\Gamma(k)\Gamma\left(N_B+\frac{1-\nu}{2-\nu}+1\right)}.$$

2) IPPP deployment:

$$\begin{aligned}M_{Z_k}(t)=&\mathbb{E}_{f(Z_k)}\left[\exp(tZ)\right]=\int\frac{(2\pi)^k}{\Gamma(k)(2-\nu)^{k-1}}\\&\times\left(\frac{2}{\alpha}\right)z^{-2/\alpha((2-\nu)k)-1}\exp\left(-\frac{2\pi}{2-\nu}z^{-2/\alpha(2-\nu)}\right)\mathrm{d}z.\end{aligned}$$

Solving both integrals directly is difficult. Instead, an equivalent solution can be obtained by calculating the m-th moment for Z_k and then deriving the MGF based on the moments.

Theorem 4: The m-th moment of Z_k is given by:

1) *BPP deployment:*

$$\mathbb{E}\left[Z_k^m\right]=\begin{cases}R^{-m\alpha/2}\frac{\Gamma(N_B+1)\Gamma\left(k-\frac{m\alpha}{2(2-\nu)}\right)}{\Gamma(k)\Gamma\left(N_B-\frac{m\alpha}{2(2-\nu)}+1\right)}, & k-\frac{m\alpha}{2(2-\nu)}\notin\mathbb{Z}_{\le0}\\\infty, & \text{otherwise}\end{cases}$$

2) *IPPP deployment:*

$$\mathbb{E}\left[Z_k^m\right]=\begin{cases}\left(\frac{\nu+2}{2\pi}\right)^{-\frac{\alpha m}{2(\nu+2)}}\frac{\Gamma\left(k-\frac{\alpha m}{2(\nu+2)}\right)}{\Gamma(k)}, & k-\frac{\alpha m}{2(\nu+2)}\notin\mathbb{Z}_{\le0}\\\infty, & \text{otherwise.}\end{cases}$$

Proof: See Appendix E □

Based on the moments, we can calculate the cumulants and moments.

Lemma 5: The first four cumulants of $Y_l|\mathbf{x}_s,\mathcal{H}_1$, κ_i, $i=1$, 2, 3, 4 are given by:

$$\begin{aligned}\kappa_1=&\sum_{k=1}^{N_B}\sqrt{P_0}\mathbb{E}\left[Z_k\right],\\\kappa_2=&\sum_{k=1}^{N_B}P_0\left(\mathbb{E}\left[Z_k^2\right]-\left(\mathbb{E}\left[Z_k\right]\right)^2\right)+\sigma_W^2,\\\kappa_3=&\sum_{k=1}^{N_B}\sqrt{P_0}^3\left(\mathbb{E}\left[Z_k^3\right]-3\mathbb{E}\left[Z_k^2\right]\mathbb{E}\left[Z_k\right]+2\left(\mathbb{E}\left[Z_k\right]\right)^3\right),\\\kappa_4=&\sum_{k=1}^{N_B}P_0^2\left(\mathbb{E}\left[Z_k^4\right]-4\mathbb{E}\left[Z_k^3\right]\mathbb{E}\left[Z_k\right]-3\left(\mathbb{E}\left[Z_k^2\right]\right)^2\right)\\&+\left(12\mathbb{E}\left[Z_k^2\right]\left(\mathbb{E}\left[Z_k\right]\right)^2-6\left(\mathbb{E}\left[Z_k\right]\right)^4\right).\end{aligned}$$

The Moments can be expressed as polynomials of cumulants:

$$\begin{aligned}\mu_1=&\kappa_1,\\\mu_2=&\kappa_2+\kappa_1^2,\\\mu_3=&\kappa_3+3\kappa_2\kappa_1+\kappa_1^3,\\\mu_4=&\kappa_4+4\kappa_3\kappa_1+3\kappa_2^2+6\kappa_2\kappa_1^2+\kappa_1^4.\end{aligned}$$

Proof: See Appendix F. □

Now that we have derived the four cumulants and moments, we use the series expansion methods in Section IV to approximate $p_{Y_l}(y|\mathbf{x}_s, \mathcal{H}_1)$ and derive the LRT in (1). Finally, the Event Detection algorithm under FBPP is presented in Algorithm 1.

Algorithm 1: Event Detection in Sensor Networks with Random Deployment

Input: Y_l, γ, N_i, R, ν, α, σ_w
Output: Binary decision ($\mathcal{H}_1$, $\mathcal{H}_0$)
1) Calculate the first four moments as per Theorem 4.
2) Calculate κ_i and μ_i according the lemma 5.
3) Perform S-K region analysis to assess the appropriateness of each of the series expansions according to Lemma 3, Lemma 4 and Theorem 3.
4) Choose the series expansion for which the S-K point is inside the S-K region.
5) Evaluate the series expansion chosen in Section IV to find $\widehat{p}_{Y_l}(y|\mathbf{x}_s, \mathcal{H}_1)$ according to (3).
6) Calculate $\Lambda(Y_l)$ via (1) and compare to the threshold γ.

VI. Simulation Results

We present the performance of the proposed algorithms via Monte Carlo simulations, where we first present the moment calculation accuracy, then the positivity regions of the estimated density and finally the detection performance via Receiver Operating Characteristics (ROC) curves. The simulations setting is as follows: the results are obtained from 50,000 realizations for a given parameter set of $N, \sigma_w, \nu, P_0, R, \alpha$. The additive noise is assumed to be i.i.d. Gaussian distributed at each sensor.

A. Moments Calculation

In Figs. 1–2, we present comparison of theoretical moments (Theorem 4) and Monte Carlo simulations for BPP and PPP. For both cases we consider both homogeneous and non-homogenous deployments. For both BPP and PPP, the results show good match with the Monte Carlo simulations as well as increased accuracy as the number of sensors increases.

B. Comparison of Critical Region

When the sensors are located close to the center of the region, the empirical sample density and estimated density do not agree. This is because those points close to the center may violate the probability density because they will result in an inaccurate sample mean. Therefore, we remove a small hole around the center. We use r to represent the radius of the hole, which we call critical region. Fig. 3 shows the effect of removing those points for different critical region sizes. In particular, we vary $r \in \{0.1, 0.5, 1, 5\}$. We also compare the accuracy of series expansion methods with respect to different r. In Fig. 3, we clearly show the effect that r has on the approximation for all three series expansion methods. In Fig. 3, we show the probability density function (PDF) for different values of r. From extensive numerical experiments, we have found that the choice $r = 5$ yields accurate approximations for a range of moments and will be used in all simulations.

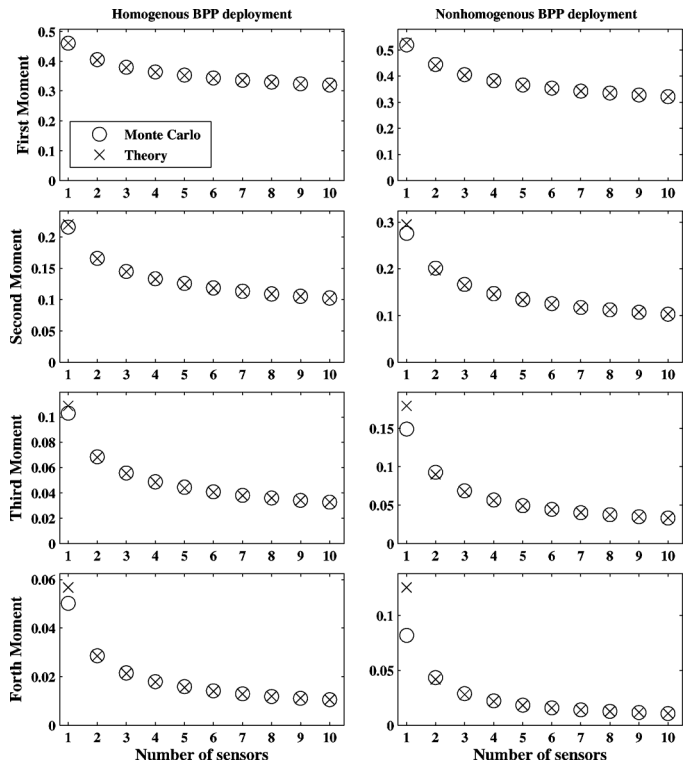

Fig. 1. Comparison of the theoretical results of the first four moments per Theorem 4 and Monte Carlo simulations under homogeneous BPP (left panel) and non-homogeneous BPP (right panel).

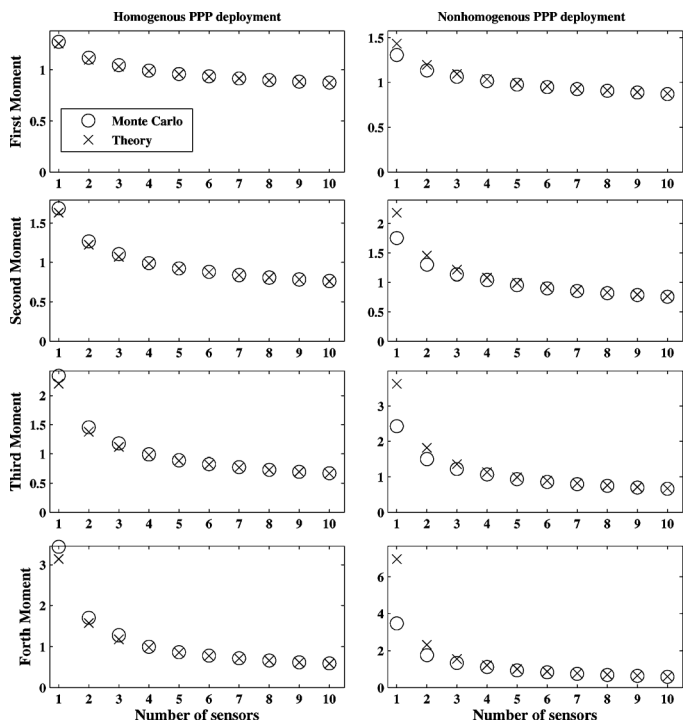

Fig. 2. Comparison of the theoretical results of the first four moments per Theorem 4 and Monte Carlo simulations under homogeneous PPP (left panel) and non-homogeneous PPP (right panel).

TABLE I
SIMULATION PARAMETERS

	Gram Charlier			Gamma Laguerre			Beta Jacobi		
Parameters	Set 1	Set 2	Set 3	Set 1	Set 2	Set 3	Set 1	Set 2	Set 3
R	100	100	100	100	100	100	100	100	100
P_0	1	1	1	1	1	1	1	1	1
N	10	10	10	50	10	10	50	10	30
α	2.5	1.7	3	2	2	3	1.7	2.3	1.5
ν	0	0	0	0	0	0.6	0	0	0.2
σ_w	1	0	0	0	0	0.4	0.8	0.4	0.8

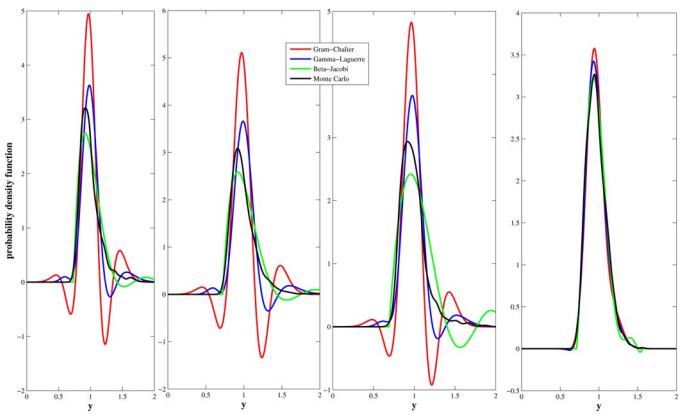

Fig. 3. Effect of critical region on marginal likelihood estimation as a function of the critical region.

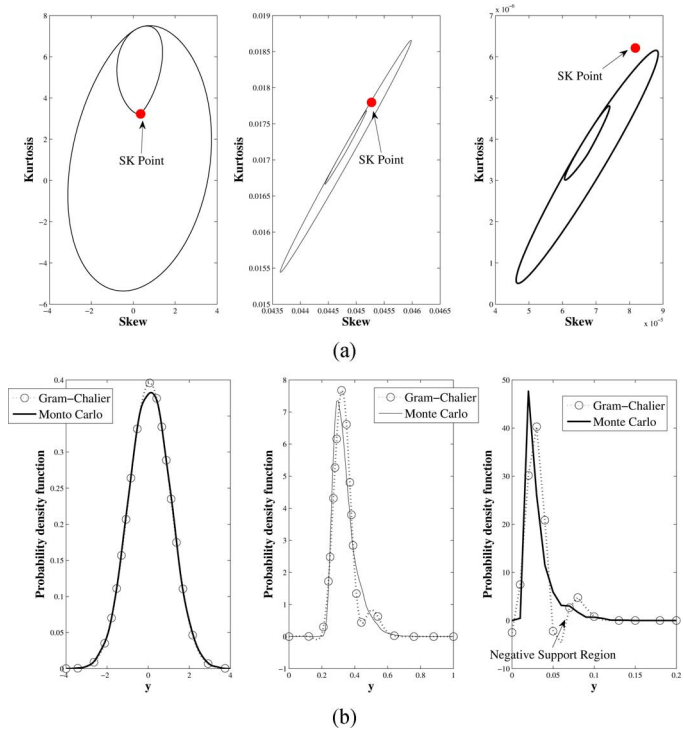

Fig. 4. Gram-Charlier series expansion for three different system parameters presented in Table I. (a) Skew-Kurtosis curves. (b) PDF estimation vs. Monte Carlo simulation.

C. Marginal Likelihood Estimation via Series Expansion and S-K Region

As discussed in Section IV, we use the Skew-Kurtosis curve to characterise regions where each of the series expansion would yield a positive PDF, given set of system parameters. It is therefore a useful tool which helps choose which series expansion to use. In this section, we present several examples to show how this will affect the approximation under each series expansion. The different sets of parameters are presented in Table I. We consider "clean signal" (i.e., $\sigma_w^2 = 0$) and "noisy signal" (i.e., $\sigma_w^2 = 0.8$), see Table I.

1) Gram-Charlier Series Expansion: In Fig. 4 we plot the S-K curve and PDF Gram-Charlier series expansion estimation for three different sets of system parameters. The three sets of system parameters generate three different Skew-Kurtosis values, represented by the red dot in each of the figures. In the left figure, the S-K point falls at the region that satisfies the conditions in Lemma 3, while the other two do not satisfy the condition, which results in poor estimation of the PDF. This illustration shows the ability of the Gram-Charlier series expansion to accurately approximate the true distribution, depending on system parameters. It is clearly shown that for noisy signal, the approximation is good, but for clean signal, the approximation has a negative PDF approximation.

2) Gamma-Laguerre Series Expansion: In Fig. 5 we plot the S-K curve and PDF Gamma-Laguerre series expansion estimation for three different sets of system parameters. In contrast with Gram-Charlier series expansion, it is clearly shown that for clean signal, the approximation is good. However, for noisy signal, the approximation is not very accurate. This is because Gamma-Laguerre series expansion only has positive support.

3) Beta-Jacobi Series Expansion: In Fig. 6 we plot the S-K curve and PDF Beta-Jacobi series expansion estimation for three different sets of system parameters. For all three cases, the approximation is accurate. The only drawback for Beta-Jacobi estimation is the small fluctuations around the tail of the density.

D. Event Detection Performance Comparison

We now present the detection performance of the algorithms via Receiver Operating characteristics (ROC) for different series expansion methods. We select one representative scenario of high noisy signal to show the direct effect of the S-K curve has on the performance of the series expansions.

In Fig. 7, we present the ROC curve for noisy signal, $\sigma_w = 0.4$ and various values of the path-loss exponent $\alpha = \{1.9, 2.1, 2.3\}$. In this case our Beta-Jacobi expansion outperforms the Gamma-Laguerre expansion and is comparable with the Gram-Chalier expansion. The system parameters are: $N = 20, \nu = 0.6, \sigma_w = 0.4, R = 100$ and we vary α from 1.9 to 2.3. It is shown that Gamma-Laguerre performs the worst

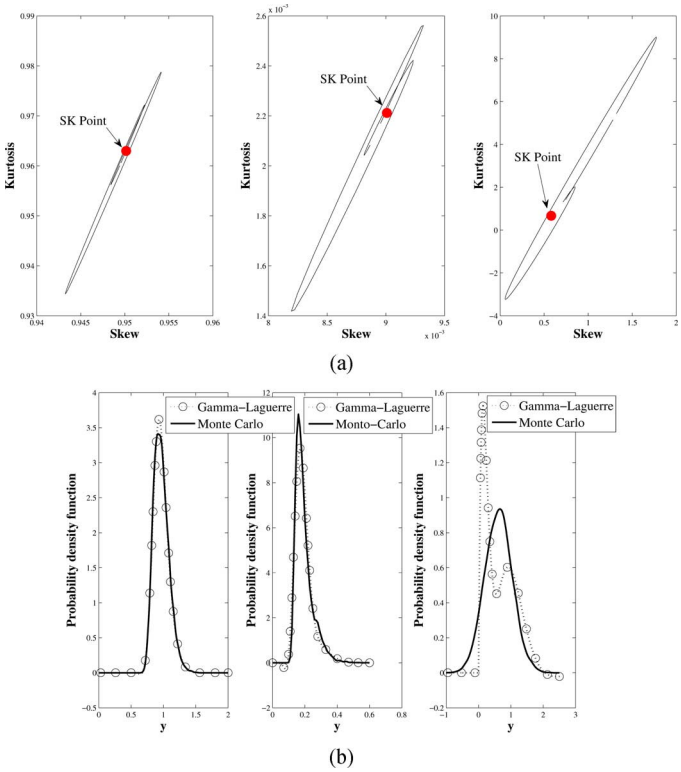

Fig. 5. Gamma-Laguerre series expansion for three different system parameters in Table I. (a) Skew-Kurtosis curves. (b) PDF estimation vs. Monte Carlo simulation.

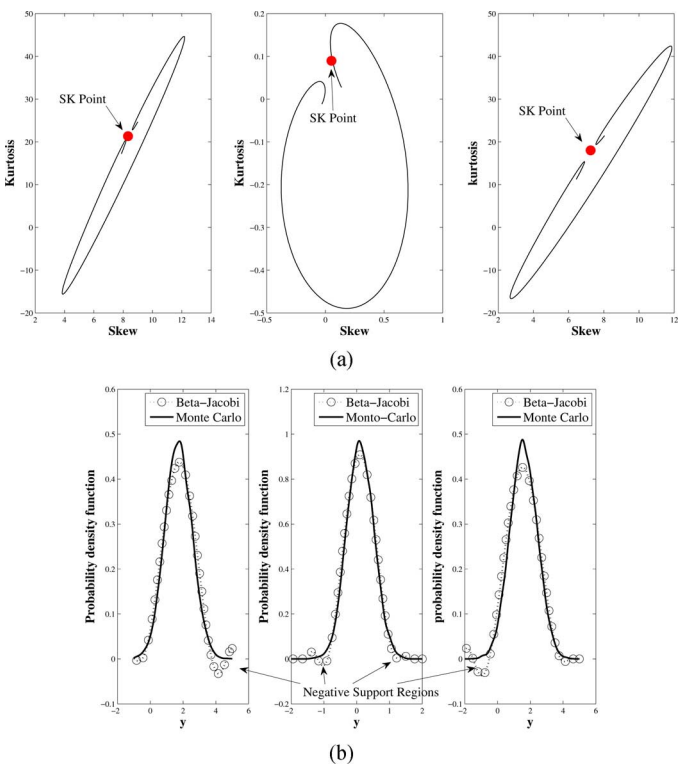

Fig. 6. Beta-Jacobi series expansion for three different system parameters in Table I. (a) Skew-Kurtosis curves. (b) PDF estimation vs. Monte Carlo simulation.

for these cases. This is because the support of the marginal density has negative values and Gamma-Laguerre can only have positive support. The same interpretation can also be found in the S-K curves.

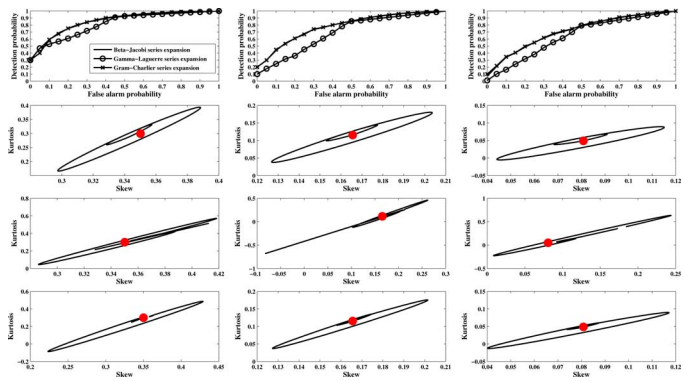

Fig. 7. ROC curves for the three series expansions for different values of path-loss exponent $\alpha = \{1.9, 2.1, 2.3\}$. The second to third rows shows the S-K curves for the three series expansion methods respectively.

The proposed Beta-Jacobi series expansion is a general scheme which is suitable for both clean and noisy signals. The advantage of using our proposed Beta-Jacobi series expansion is that it performs at least as well as the other series expansions **in any system parameter values**, as depicted in Fig. 7. This means that the Beta-Jacobi series expansion replaces the need to work with two different series expansions and eliminates the need to decide at which system parameters (such as signal and noise values, path-loss exponent, deployment size etc.) to switch from one expansion to the other. One important contribution we are making in this regard is the development of an analysis tool which is based on the Skew-Kurtosis of each expansion and provide the statistical interpretation why the other expansions cause detection performance degradation, since they do not fulfill the positive support condition of the probability density function.

The effect of the frame length L on the ROC performance is shown in Fig. 8. This clearly shows that increasing number of observations delivers improved detection performance, especially for low false alarm rate.

VII. Conclusions

In this paper, an event detection algorithms in Wireless Sensor Networks was developed under two types of random spatial deployments. A binary hypothesis testing problem was formulated and optimal decision rule was designed for it. The marginal densities under two hypothesis were derived. We used simple yet accurate series expansion methods to approximate the marginal density under alternative hypothesis. The various series expansion methods were practical and suitable for different practical scenarios. We also used extensive simulation results to generate the Receiver Operating Curves (ROC) under different sets of parameters. The optimality of the series expansion methods was verified and the Skew-Kurtosis Curves were shown for each method. Our schemes provided useful benchmark for other centralized and distributed scheme designs.

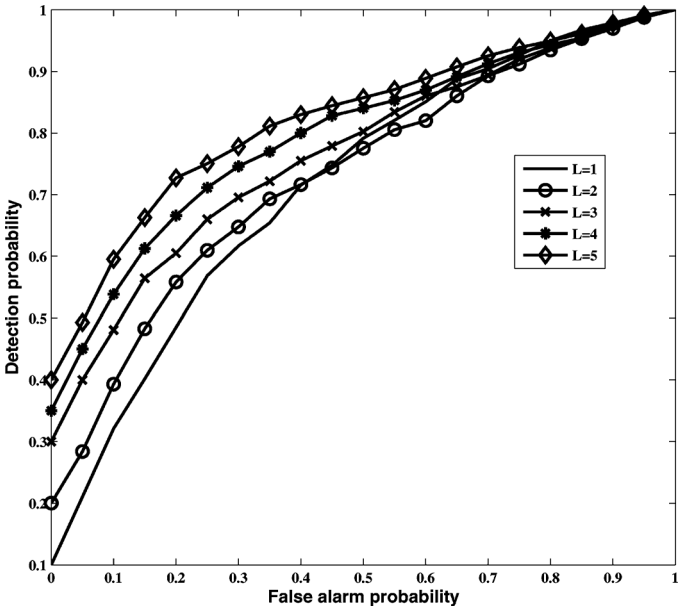

Fig. 8. Effect of different number of time frames on the ROC performance using Beta-Jacobi series expansion for Low SNR case ($\alpha = 2.3, \sigma_w = 0.4, \nu = 0.6, N = 20$).

Appendix A
Proof of Theorem 1

Proof: We begin by calculating p, as defined in Definition 1. According to [39], assume that $b_d(x,r)$ is contained within W and W is circle with Radius R. We then obtain that

$$p = \int_{b_d x, r \cap W} \lambda(x)\mathrm{d}x = \frac{\int_{b_d(x,r)} \lambda(x)\mathrm{d}x}{\int_W \lambda(x)\mathrm{d}x} = \frac{\int_0^r x^{-\nu} 2\pi x \mathrm{d}x}{\int_0^R x^{-\nu} 2\pi x \mathrm{d}x} = \begin{cases} \left(\frac{r}{R}\right)^{2-\nu}, & \nu < 2 \\ \frac{\log r - \log \varepsilon}{\log R - \log \varepsilon}, & \nu = 2 \\ \frac{r^{2-\nu} - \varepsilon^{2-\nu}}{R^{2-\nu} - \varepsilon^{2-\nu}}, & \nu > 2, \end{cases}$$

where $\varepsilon \to 0^+$.

Next, utilizing the results in [39], we can find the general expression for distribution distribution under inhomogeneous deployment. The procedure is same except that we use the expression for p from the above equation. For BPP, N_B is finite number. For IPPP, N_P is asymptotically $+\infty$. we obtain the following:

BPP deployment:

$$\begin{aligned} f_{R_k}(r|\mathbf{x}_s, \mathcal{H}_1) &= \frac{\mathrm{d}p}{\mathrm{d}r} \frac{(1-p)^{N_B-k} p^{k-1}}{B(N_B-k+1,k)} \\ &= \frac{2-\nu}{R} \frac{(1-p)^{N_B-k} p^{k-1+\frac{1-\nu}{2-\nu}}}{B(N_B-k+1,k)} \\ &= \frac{2-\nu}{R} \frac{\Gamma\left(k+\frac{1-\nu}{2-\nu}\right)\Gamma(N_B+1)}{\Gamma(k)\Gamma\left(N_B+\frac{1-\nu}{2-\nu}+1\right)} \\ &\quad \times \beta\left(\left(\frac{r}{R}\right)^{2-\nu}; k+\frac{1-\nu}{2-\nu}, N_B-k+1\right). \end{aligned}$$

IPPP deployment:

$$\begin{aligned} f_{R_k}(r|\mathbf{x}_s, \mathcal{H}_1) &= \frac{2-\nu}{R} \frac{(1-p)^{N_P-k} p^{k-1+\frac{1-\nu}{2-\nu}}}{B(N_P-k+1,k)} \\ &= \frac{2-\nu}{R} \frac{(1-p)^{N_P-k} p^{k-1+\frac{1-\nu}{2-\nu}} \Gamma(N_P+1)}{\Gamma(N_P-k+1)\Gamma(k)}. \end{aligned}$$

□

Appendix B
Proof of Lemma 1

Proof: We utilize the results for transformation of random variables to obtain:

BPP deployment:

$$\begin{aligned} f_{Z_k}(z) &= -f\left(\phi^{-1}(z)\right) \frac{\mathrm{d}\phi^{-1}(z)}{\mathrm{d}z} \\ &= \frac{2(2-\nu)}{R\alpha} \frac{\Gamma\left(k+\frac{1-\nu}{2-\nu}\right)\Gamma(N_B+1)}{\Gamma(k)\Gamma\left(N_B+\frac{1-\nu}{2-\nu}+1\right)} z^{-2/\alpha-1} \\ &\quad \times \beta\left(\left(\frac{z^{-2/\alpha}}{R}\right)^{2-\nu}; k+\frac{1-\nu}{2-\nu}, N_B-k+1\right) \end{aligned}$$

IPPP deployment:

Let $z = \phi(r) = r^{-\alpha/2}$, $y \in (0,\infty)$. Then

$$\begin{aligned} f_{Z_k}(z) &= -f_{R_k}\left(\phi^{-1}(z)\right) \frac{d\phi^{-1}(z)}{\mathrm{d}z} \\ &= \frac{(2\pi)^k}{\Gamma(k)(2-\nu)^{k-1}} \left(\frac{2}{\alpha}\right) z^{-2/\alpha((2-\nu)k)-1} \\ &\quad \times \exp\left(\frac{2\pi}{2-\nu} z^{-2/\alpha(2-\nu)}\right). \end{aligned}$$

□

Appendix C
Proof of Theorem 2

Proof: To obtain the coefficients a_i, we need to solve the following expression:

$$a_i = \frac{B(\theta,\eta)(2i+\theta+\eta-1)\Gamma(i+\theta+\eta-1)i!}{\Gamma(i+\theta)\Gamma(i+\eta)} \times \int_{-1}^{1} f(x) P_i^{(\eta-1,\theta-1)}(x)\,\mathrm{d}x.$$

Using the following series expansion:

$$\left(\frac{x-1}{2}\right)^m = \frac{1}{2^m} \sum_{j=0}^{m} \binom{m}{j} (-1)^{m-j} x^j \mathrm{d}x,$$

and after some algebraic manipulations, we obtain that

$$a_i = \sum_{j=0}^{i} \mu_j \frac{B(\theta,\eta)(2i+\theta+\eta-1)i!}{\Gamma(i+\theta)} \times \sum_{m=j}^{i} \frac{\Gamma(\theta+\eta+i+m-1)}{\Gamma(i-m+1)\Gamma(\eta+m)m!2^m} \binom{m}{j} (-1)^{m-j}.$$

where $\mu_j = \mathbb{E}\left[X^j\right] = \int_{-1}^{1} f(x) x^j \mathrm{d}x$. □

APPENDIX D
PROOF OF THEOREM 3

Proof: We express the fourth order Beta-Jacobi series expansion as follows:

$$\begin{aligned} f(x) &= \frac{(x+1)^{\theta-1}(1-x)^{\eta-1}}{B(\theta,\eta)2^{\theta+\eta-1}} \sum_{i=0}^{4} a_i P_i^{(\eta-1,\theta-1)}(x) \\ &= B_1\mu_3 + B_2\mu_4 + B_3, \end{aligned}$$

where

$$\begin{aligned} B_1 &= (C_{33}P_3 + C_{43}P_4)\frac{(x+1)^{\theta-1}(1-x)^{\eta-1}}{B(\theta,\eta)2^{\theta+\eta-1}}, \\ B_2 &= C_{44}P_4\frac{(x+1)^{\theta-1}(1-x)^{\eta-1}}{B(\theta,\eta)2^{\theta+\eta-1}}, \\ B_3 &= \frac{(x+1)^{\theta-1}(1-x)^{\eta-1}}{B(\theta,\eta)2^{\theta+\eta-1}}\left((C_{30}+C_{31}\mu_1+C_{32}\mu_2)P_3\right) \\ &\quad + \frac{(x+1)^{\theta-1}(1-x)^{\eta-1}}{B(\theta,\eta)2^{\theta+\eta-1}} \\ &\quad \cdot \left(\sum_{i=0}^{2} a_i P_i + (C_{40}+C_{41}\mu_1+C_{42}\mu_2)P_4\right), \\ C_{ij} &= \frac{B(\theta,\eta)(2i+\theta+\eta-1)\,i!}{\Gamma(i+\theta)} \sum_{m=j}^{i} \binom{m}{j}(-1)^{m-j} \\ &\quad \times \frac{\Gamma(\eta+\theta+i+m-1)}{\Gamma(i-m+1)\Gamma(\eta+m)\,m!2^m}, \end{aligned}$$

and $\mu_1 = \mathbb{E}[X], \mu_2 = \mathbb{E}[X^2]$.

In order to guarantee that $f(x)$ is positive, we obtain the following set of equations

$$\begin{cases} B_1\mu_3 + B_2\mu_4 + B_3 = 0, & (f(x)=0) \\ B_1'\mu_3 + B_2'\mu_4 + B_3' = 0, & (f'(x)=0) \end{cases} \quad \text{for } x \in [-1,1]$$

Solving for the Skew and Kurtosis, we obtain that:

$$\begin{cases} \mu_3(x) = -\frac{1}{B_1}(\mu_4(x)B_2 + B_3) \\ \mu_4(x) = \left(\frac{B_1'B_3}{B_1} - B_3'\right)\left(B_2' - \frac{B_1'B_2}{B_1}\right)^{-1}, \end{cases}$$
$$\text{for;} \quad x \in [-1,+1)$$

where

$$\begin{aligned} B_1' &= (C_{33}P_3' + C_{43}P_4')\frac{(x+1)^{\theta-1}(1-x)^{\eta-1}}{B(\theta,\eta)2^{\theta+\eta-1}} \\ &\quad + B_1\left(\frac{\theta+1}{x+1} - \frac{\eta-1}{1-x}\right), \\ B_2' &= C_{44}P_4'\frac{(x+1)^{\theta-1}(1-x)^{\eta-1}}{B(\theta,\eta)2^{\theta+\eta-1}} + B_2\left(\frac{\theta+1}{x+1} - \frac{\eta-1}{1-x}\right), \\ B_3' &= \sum_{i=0}^{2} a_i P_i' + (C_3 + C_{31}\mu_1 + C_{32}\mu_2)P_3' \\ &\quad + (C_4 + C_{41}\mu_1 + C_{42}\mu_2)P_4'\frac{(x+1)^{\theta-1}(1-x)^{\eta-1}}{B(\theta,\eta)2^{\theta+\eta-1}} \\ &\quad + B_3\left(\frac{\theta+1}{x+1} - \frac{\eta-1}{1-x}\right), \end{aligned}$$

and

$$\begin{aligned} P_0' &= 0 \\ P_i' &= \frac{\Gamma(\eta+i)}{\Gamma(\eta+\theta+i-1)} \\ &\quad \times \left(\sum_{m=1}^{i} \frac{\Gamma(\eta+\theta+i+m-1)}{2\Gamma(i-m+1)\Gamma(\eta+m)(m-1)!}\left(\frac{x-1}{2}\right)^{m-1}\right). \end{aligned}$$

□

APPENDIX E
PROOF OF THEOREM 4

Proof:

1) BPP deployment:
We define the following change of variables: $X = \left(\frac{Z^{-2/\alpha}}{R}\right)^{2-\nu}$. We express the m-th moment of Z_k:

$$\begin{aligned} \mathbb{E}[Z_k^m] &= \int w(k)\beta\left(x; k+\frac{1-\nu}{2-\nu}, N_B-k+1\right) \\ &\quad \times \left(x^{-\frac{\alpha}{2(2-\nu)}}R^{-\alpha/2}\right)^{-\frac{2}{\alpha}+m-1} \frac{\mathrm{d}x^{-\frac{\alpha}{2(2-\nu)}}R^{-\alpha/2}}{\mathrm{d}x}\mathrm{d}x \\ &= C_1\int_0^1 \frac{1}{B\left(k+\frac{1-\nu}{2-\nu}, N_B-k+1\right)} x^{k-\frac{m\alpha}{2(2-\nu)}-1} \\ &\quad \times (1-x)^{N_B-k}\,\mathrm{d}x \\ &= C_1\frac{B\left(k-\frac{m\alpha}{2(2-\nu)}, N_B-k+1\right)}{B\left(k+\frac{1-\nu}{2-\nu}, N_B-k+1\right)}, \end{aligned}$$

where $B(\cdot)$ is the β function and

$$C_1 = R^{-m\alpha/2}\frac{\Gamma\left(k+\frac{1-\nu}{2-\nu}\right)\Gamma(N_B+1)}{\Gamma(k)\Gamma\left(N_B+\frac{1-\nu}{2-\nu}+1\right)}.$$

Finally we obtain that

$$\mathbb{E}\left[Z_{k_l}^m\right] = R^{-m\alpha/2}\frac{\Gamma(N_B+1)\Gamma\left(k-\frac{m\alpha}{2(2-\nu)}\right)}{\Gamma(k)\Gamma\left(N_B-\frac{m\alpha}{2(2-\nu)}+1\right)}.$$

2) IPPP deployment: We express the m-th moment:

$$\begin{aligned} \mathbb{E}[Z_k^m] &= \int_0^\infty z^m f_{Z_k}(z)\mathrm{d}z \\ &= \frac{2}{\alpha}\frac{(2\pi)^k}{\Gamma(k)(2-\nu)^{k-1}}\int_0^\infty z^{m-2(2-\nu)k/\alpha-1} \\ &\quad \times \exp\left(-\frac{2\pi}{2-\nu}z^{-2/\alpha(c+2)}\right)\mathrm{d}z. \end{aligned}$$

Using the identity $\Gamma(t) = \int_0^\infty x^{t-1}\exp^{-x}\mathrm{d}x$, and the following change of variables $X = \frac{2\pi}{c+2}Z^{-2/\alpha(2-\nu)}$, we obtain that

$$\begin{aligned} \mathbb{E}[Z_k^m] &= \frac{2}{\alpha}\frac{(2\pi)^k}{\Gamma(k)(2-\nu)^{k-1}}\frac{\alpha}{2(2-\nu)}\left(\frac{2-\nu}{2\pi}\right)^{-\frac{\alpha m}{2(2-\nu)}+k} \\ &\quad \times \int_0^{+\infty}\exp(-x)\,x^{k-\frac{\alpha m}{2(2-\nu)}-1}\mathrm{d}x \\ &= \left(\frac{2-\nu}{2\pi}\right)^{-\frac{\alpha m}{2(2-\nu)}}\frac{\Gamma\left(k-\frac{\alpha m}{2(2-\nu)}\right)}{\Gamma(k)}. \end{aligned}$$

□

APPENDIX F
PROOF OF LEMMA 5

Proof:

1) BPP deployments:
Using the result in Theorem 4, MGF of Z_k is given by:

$$M_{Z_k}(t) = 1+\sum_{m=1}^{\infty} \frac{t^m}{m!} R^{-m\alpha/2} \frac{\Gamma(N_B+1)\Gamma\left(k-\frac{m\alpha}{2(2-\nu)}\right)}{\Gamma(k)\Gamma\left(N_B-\frac{m\alpha}{2(2-\nu)}+1\right)}$$

Due to the conditional independence of Z_k, and that the MGF of W_l is given by $M_{W_l}(t) = \exp\left(\frac{1}{2}\sigma_{w_l}^2 t^2\right)$, we have that

$$M_{Y_l}(t) = \prod_{k=1}^{N_B} M_{Z_k}(t) M_{W_l}(t) = \prod_{k=1}^{N_B} \left(1+\sum_{m=1}^{\infty} \frac{(\sqrt{P_0}t)^m}{m!} R^{-m\alpha/2} \frac{\Gamma(N_B+1)\Gamma\left(k-\frac{m\alpha}{2(2-\nu)}\right)}{\Gamma(k)\Gamma\left(N_B-\frac{m\alpha}{2(2-\nu)}+1\right)}\right) \times \mathrm{e}^{\frac{1}{2}\sigma_W^2 t^2}.$$

2) IPPP deployments:
Using the result in Theorem 4, MGF of Z_k is given by:

$$M_{Z_k}(t) = 1+\sum_{m=1}^{\infty} \frac{t^m}{m!} \left(\frac{2-\nu}{2\pi}\right)^{-\frac{\alpha m}{2(2-\nu)}} \frac{\Gamma\left(k-\frac{\alpha m}{2(2-\nu)}\right)}{\Gamma(k)}$$

Using the same procedure as before, we obtain that

$$M_{Y_l}(t) = \prod_{k=1}^{N_P} \left(1+\sum_{m=1}^{\infty} \frac{(\sqrt{P_0}t)^m}{m!} \left(\frac{2-\nu}{2\pi}\right)^{-\frac{\alpha m}{2(2-\nu)}} \frac{\Gamma\left(k-\frac{\alpha m}{2(2-\nu)}\right)}{\Gamma(k)}\right) \times \sigma_W^2 t^2.$$

In order to derive cumulants and moments, first we find the cumulant function $g(t)$ under both deployments.

1) BPP deployment:

$$g(t) = \log M_{Y_l}(t) = \sum_{k=1}^{N_B} \log\left(1+\sum_{m=1}^{\infty} \frac{(\sqrt{P_0}t)^m}{m!} R^{-\frac{\alpha}{2}m} h(k)\right) + \frac{1}{2}\sigma_w^2 t^2,$$

where

$$h(k) := R^{-m\alpha/2} \frac{\Gamma(N_B+1)\Gamma\left(k-\frac{m\alpha}{2(2-\nu)}\right)}{\Gamma(k)\Gamma\left(N_B-\frac{m\alpha}{2(2-\nu)}+1\right)}.$$

Next we obtain the first cumulant κ_1 as follows:

$$\kappa_1 = \left.\frac{\mathrm{d}g(t)}{\mathrm{d}t}\right|_{t=0} = \sum_{k=1}^{N_B} \left.\frac{\frac{\sqrt{P_0}t^0}{1}h(k) + \sum_{m=2}^{\infty} m\frac{(\sqrt{P_0})^m t^{m-1}}{m!}h(k)}{1+\sum_{m=1}^{\infty}\frac{(\sqrt{P_0}t)^m}{m!}h(k)}\right|_{t=0} + \sigma_W^2 t|_{t=0} = \sum_{k=1}^{N_B} \sqrt{P_0}h(k) = \sum_{k=1}^{N_B} \sqrt{P_0}\mathbb{E}[Z_k].$$

Similarly, by taking the second, third and forth derivative of $g(t)$. We next find the κ_2, κ_3 and κ_4 as shown in Theorem 5.

2) IPPP deployment:
κ_1, κ_2, κ_3 and κ_4 are in the same form as those in BPP deployment using the appropriate values for the moments. □

REFERENCES

[1] A. Kottas, Z. Wang, and A. Rodríguez, "Spatial modeling for risk assessment of extreme values from environmental time series: A Bayesian nonparametric approach," *Environmetrics*, vol. 23, no. 8, pp. 649–662, 2012.

[2] J. P. French and S. R. Sain, "Spatio-temporal exceedance locations and confidence regions," *Ann. Appl. Statist.*, 2013, to be published.

[3] I. Akyildiz, W. Su, Y. Sankarasubramaniam, and E. Cayirci, "Wireless sensor networks: A survey," *Comput. Netw.*, vol. 38, no. 4, pp. 393–422, 2002.

[4] G. Anastasi, M. Conti, M. Di Francesco, and A. Passarella, "Energy conservation in wireless sensor networks: A survey," *Ad Hoc Netw.*, vol. 7, no. 3, pp. 537–568, 2009.

[5] F. Fazel, M. Fazel, and M. Stojanovic, *Random Access Sens. Netw.: Field Reconstruct. Incomplete Data*, pp. 300–305, 2012.

[6] J. Matamoros, F. Fabbri, C. Antón-Haro, and D. Dardari, "On the estimation of randomly sampled 2D spatial fields under bandwidth constraints," *IEEE Trans. Wireless Commun.*, vol. 10, no. 12, pp. 4184–4192, 2011.

[7] B. Krishnamachari and S. Iyengar, "Distributed Bayesian algorithms for fault-tolerant event region detection in wireless sensor networks," *IEEE Trans. Comput.*, vol. 53, no. 3, pp. 241–250, 2004.

[8] P. Dutta, M. Grimmer, A. Arora, S. Bibyk, and D. Culler, "Design of a wireless sensor network platform for detecting rare, random, and ephemeral events," in *Proc. 4th Int. Symp. Inf. Process. Sens. Netw.*, 2005, p. 70.

[9] W. Bajwa, A. Sayeed, and R. Nowak, "Matched source-channel communication for field estimation in wireless sensor networks," in *Proc. 4th Int. Symp. Inf. Process. Sens. Netw.*, 2005, p. 44.

[10] A. Nordio, C.-F. Chiasserini, and E. Viterbo, "Performance of linear field reconstruction techniques with noise and uncertain sensor locations," *IEEE Trans. Signal Process.*, vol. 56, no. 8, pp. 3535–3547, 2008.

[11] J. W. Branch, C. Giannella, B. Szymanski, R. Wolff, and H. Kargupta, "In-network outlier detection in wireless sensor networks," *Knowl. Inf. Syst.*, vol. 34, no. 1, pp. 23–54, 2013.

[12] Y. Zhang, N. Meratnia, and P. Havinga, "Outlier detection techniques for wireless sensor networks: A survey," *IEEE Commun. Surv. Tutor.*, vol. 12, no. 2, pp. 159–170, 2010.

[13] G. Mao, B. Fidan, and B. D. Anderson, "Wireless sensor network localization techniques," *Comput. Netw.*, vol. 51, no. 10, pp. 2529–2553, 2007.

[14] P. Biswas and Y. Ye, "Semidefinite programming for ad hoc wireless sensor network localization," in *Proc. 3rd Int. Symp. Inf. Process. Sens. Netw.*, 2004, pp. 46–54.

[15] R. Viswanathan and P. K. Varshney, "Distributed detection with multiple sensors I. Fundamentals," *Proc. IEEE*, vol. 85, no. 1, pp. 54–63, 1997.

[16] J.-J. Xiao and Z.-Q. Luo, "Universal decentralized detection in a bandwidth-constrained sensor network," *IEEE Trans. Signal Process.*, vol. 53, no. 8, pp. 2617–2624, 2005.
[17] T. Aysal and K. Barner, "Constrained decentralized estimation over noisy channels for sensor networks," *IEEE Trans. Signal Process.*, vol. 56, no. 4, pp. 1398–1410, 2008.
[18] M. Zhu, S. Ding, Q. Wu, R. R. Brooks, N. S. Rao, and S. S. Iyengar, "Fusion of threshold rules for target detection in wireless sensor networks," *ACM Trans. Sens. Netw. (TOSN)*, vol. 6, no. 2, p. 18, 2010.
[19] M. Guerriero, L. Svensson, and P. Willett, "Bayesian data fusion for distributed target detection in sensor networks," *IEEE Trans. Signal Process.*, vol. 58, no. 6, pp. 3417–3421, 2010.
[20] J.-F. Chamberland and V. V. Veeravalli, "Wireless sensors in distributed detection applications," *IEEE Signal Process. Mag.*, vol. 24, no. 3, pp. 16–25, 2007.
[21] P. Karumbu, V. K. Prasanthi, and A. Kumar, "Delay optimal event detection on ad hoc wireless sensor networks," *ACM Trans. Sens. Netw. (TOSN)*, vol. 8, no. 2, p. 12, 2012.
[22] D. Bajovic, B. Sinopoli, and J. Xavier, "Sensor selection for event detection in wireless sensor networks," *IEEE Trans. Signal Process.*, vol. 59, no. 10, pp. 4938–4953, 2011.
[23] D. Ciuonzo, G. Romano, and P. Rossi, "Performance analysis and design of maximum ratio combining in channel-aware MIMO decision fusion," *IEEE Trans. Wireless Commun.*, vol. 12, no. 9, pp. 4716–4728, 2013.
[24] I. Nevat, G. W. Peters, and I. Collings, "Distributed detection in sensor networks over fading channels with multiple antennas at the fusion centre," *IEEE Trans. Signal Process.*, vol. 62, no. 3, pp. 671–683, 2014.
[25] X. Zhang, H. Poor, and M. Chiang, "Optimal power allocation for distributed detection over MIMO channels in wireless sensor networks," *IEEE Trans. Signal Process.*, vol. 56, no. 9, pp. 4124–4140, 2008.
[26] P. Zhang, J. Y. Koh, S. Lin, and I. Nevat, *Distributed Event Detection under Byzantine Attack in Wireless Sensor Networks*. New York, NY, USA: IEEE, 2014, pp. 1–6.
[27] R. Niu and P. K. Varshney, "Performance analysis of distributed detection in a random sensor field," *IEEE Trans. Signal Process.*, vol. 56, no. 1, pp. 339–349, 2008.
[28] A. Dogandzic and B. Zhang, "Distributed estimation and detection for sensor networks using hidden Markov random field models," *IEEE Trans. Signal Process.*, vol. 54, no. 8, pp. 3200–3215, 2006.
[29] Y. Chen, "Modeling information flows in distributed sensor networks: Chernoff information azimuth spectrum," *IEEE Trans. Signal Process.*, vol. 60, no. 9, pp. 4898–4912, Sep. 2012.
[30] G. Werner-Allen, K. Lorincz, M. Ruiz, O. Marcillo, J. Johnson, J. Lees, and M. Welsh, "Deploying a wireless sensor network on an active volcano," *IEEE Internet Comput.*, vol. 10, no. 2, pp. 18–25, 2006.
[31] G. Werner-Allen, K. Lorincz, J. Johnson, J. Lees, and M. Welsh, "Fidelity and yield in a volcano monitoring sensor network," in *Proc. 7th Symp. Operat. Syst. Design Implement.*, 2006, pp. 381–396.
[32] G. Werner-Allen, J. Johnson, M. Ruiz, J. Lees, and M. Welsh, "Monitoring volcanic eruptions with a wireless sensor network," in *Proc. 2nd Eur. Workshop Wireless Sens. Netw.*, 2005, pp. 108–120.
[33] W.-Z. Song, R. Huang, M. Xu, A. Ma, B. Shirazi, and R. LaHusen, "Air-dropped sensor network for real-time high-fidelity volcano monitoring," in *Proc. 7th Int. Conf. on Mobile Syst., Appl., Serv.*, 2009, pp. 305–318.
[34] S. M. Brennan, A. M. Mielke, D. C. Torney, and A. B. MacCabe, "Radiation detection with distributed sensor networks," *Computer*, vol. 37, no. 8, pp. 57–59, 2004.
[35] J. Barbarán, M. Díaz, I. Esteve, and B. Rubio, "Radmote: A mobile framework for radiation monitoring in nuclear power plants," *Int. J. Electron. Circuits Syst.*, vol. 1, pp. 104–109, 2007.
[36] F. Ding, G. Song, K. Yin, J. Li, and A. Song, "A GPS-enabled wireless sensor network for monitoring radioactive materials," *Sens. Actuators A: Phys.*, vol. 155, no. 1, pp. 210–215, 2009.
[37] J. G. Andrews, F. Baccelli, and R. K. Ganti, "A tractable approach to coverage and rate in cellular networks," *IEEE Trans. Commun.*, vol. 59, no. 11, pp. 3122–3134, 2011.
[38] J. G. Andrews, R. K. Ganti, M. Haenggi, N. Jindal, and S. Weber, "A primer on spatial modeling and analysis in wireless networks," *IEEE Commun. Mag.*, vol. 48, no. 11, pp. 156–163, 2010.
[39] M. Haenggi, "On distances in uniformly random networks," *IEEE Trans. Inf. Theory*, vol. 51, no. 10, pp. 3584–3586, Oct. 2005.
[40] D. Moltchanov, "Distance distributions in random networks," *Ad Hoc Netw.*, vol. 10, no. 6, pp. 1146–1166, 2012.
[41] H. ElSawy, E. Hossain, and M. Haenggi, "Stochastic geometry for modeling, analysis, and design of multi-tier and cognitive cellular wireless networks: A survey," *IEEE Commun. Surv. Tutor.*, vol. 15, no. 3, pp. 996–1019, 2013.
[42] Z. Gong and M. Haenggi, "Interference and outage in mobile random networks: Expectation, distribution, and correlation," *IEEE Trans. Mobile Comput.*, vol. 13, no. 2, pp. 337–349, 2014.
[43] J.-F. Chamberland and V. V. Veeravalli, "How dense should a sensor network be for detection with correlated observations?," *IEEE Trans. Inf. Theory*, vol. 52, no. 11, pp. 5099–5106, 2006.
[44] E. Jondeau and M. Rockinger, "Gram Charlier densities," *J. Econom. Dyn. Contr.*, vol. 25, no. 10, pp. 1457–1483, 2001.
[45] R. S. Targino, G. W. Peters, G. Sofronov, and P. V. Shevchenko, "Optimal insurance purchase strategies via optimal multiple stopping times," 2013 [Online]. Available: arXiv:1312.0424, to be published
[46] S. Srinivasa and M. Haenggi, "Distance distributions in finite uniformly random networks: Theory and applications," *IEEE Trans. Vehi. Technol.*, vol. 59, no. 2, pp. 940–949, Feb. 2010.
[47] A. Baddeley, "Spatial point processes and their applications," *Stochastic Geometry*, vol. 1892, pp. 1–75, 2007.
[48] H. Van Trees, *Detection, Estimation, and Modulation Theory.. Part 1,. Detection, Estimation, and Linear Modulation Theory*. New York, NY, USA: Wiley, 1968.
[49] S. Kay, *Fundamentals of Statistical Signal Processing, Volume 2: Detection Theory*. Englewood Cliffs, NJ, USA: Prentice-Hall PTR, 1998.
[50] R. Askey and J. A. Wilson, *Some basic Hypergeometric Orthogonal Polynomials that Generalize Jacobi Polynomials*. New York, NY, USA: Amer. Math. Soc., 1985, vol. 319.
[51] M. G. Cruz, G. W. Peters, and P. V. Shevchenko, *Fundamental Aspects of Operational Risk and Insurance Analytics*. New York, NY, USA: Wiley, 2014.

Pengfei Zhang received the B.Eng. degree in electrical and electronic engineering and the Ph.D. degree from Nanyang Technological University in 2010 and 2015, under supervision of Prof. Xiao Gaoxi and Prof. Tan Hwee Pink, respectively.

He is now a Research Scientist with the Institute for Infocomm Research, under the Sense-Sense-abilities Programme. His research interests include energy efficient clustering algorithms, energy harvesting wireless sensor networks (EH-WSN), and statistical modeling in WSN.

Ido Nevat received the B.Sc. degree in electrical engineering from the Technion-Israel Institute of Technology, Haifa, in 1998 and the Ph.D. degree in electrical engineering from the University of NSW, Sydney, Australia, in 2010.

From 2010 to 2013, he was a Research Fellow with the Wireless and Networking Technologies Laboratory, CSIRO, Australia. Currently he is a scientist with the Institute for Infocomm Research (I2R), Singapore. His main areas of interests include statistical signal processing and Bayesian statistical modeling.

Gareth W. Peters received the B.Sc. and B.Eng. (first Hons.) in mathematics and electrical engineering from The University of Melbourne, Victoria, Australia, the M.Sc. from the University of Cambridge, U.K., and the Ph.D. degree in Statistics from the University of NSW, Sydney, Australia in 2010. He is currently Assistant Professor in the Department of Statistical Science, Principle Investigator in Computational Statistics and Machine Learning, and Academic Member of the UK PhD Center of Financial Computing at University College London. Dr. Peters received the PhD. He is also Adjunct Scientist in the Commonwealth Scientific and Industrial Research Organisation (CSIRO), Australia; Associate

Member of Oxford-Man Institute at Oxford University; and Associate Member in the Systemic Risk Center of the London School of Economics. He set up and runs the financial risk and insurance modelling group at UCL and has published two research books and edited 3 research books as well as publishing more than 40 peer reviewed journal papers and 50 peer reviewed conference papers.

Gaoxi Xiao (M'99) received the B.S. and M.S. degrees in applied mathematics from Xidian University, Xi'an, China, in 1991 and 1994 respectively. In 1998, he received the Ph.D. degree in computing from the Hong Kong Polytechnic University.

He was an Assistant Lecturer with Xidian University during 1994–1995. He was a Postdoctoral Research Fellow in Polytechnic University, Brooklyn, New York in 1999; and a Visiting Scientist with the University of Texas at Dallas during 1999–2001. He joined the School of Electrical and Electronic Engineering, Nanyang Technological University, Singapore, in 2001, where he is now an Associate Professor. His research interests include complex systems and networks, optical and wireless networking, smart grid, system resilience, and Internet technologies.

Hwee-Pink Tan (SM'14) received the Ph.D. degree from the Technion, Israel Institute of Technology, Israel, in August 2004. In December 2004, he was awarded the A*STAR International Postdoctoral Fellowship.

He is currently an Associate Professor of Information Systems (Practice) at the Singapore Management University. He also holds the concurrent appointment of Academic Director of the SMU-TCS iCity Lab at SMU. Prior to joining SMU in March 2015, he was a Senior Scientist at the Institute of Infocomm Research (I2R), A*STAR and was also the SERC Programme Manager for the A*STAR Sense and Sense-abilities Program, where he led a team of 30 full-time research scientists and engineers. From December 2004 to June 2006, he was a Postdoctoral Researcher with EURANDOM, Eindhoven University of Technology, the Netherlands. He was a Research Fellow with The Telecommunications Research Centre (CTVR), Trinity College Dublin, Ireland, between July 2006 and March 2008. His research has focused on the design, modeling and performance evaluation of underwater acoustic sensor networks, wireless sensor networks powered by ambient energy harvesting as well as large scale and heterogeneous sensor networks. He has published more than 100 papers. His current research interests are in the design, and evaluation of Internet-of-Things and sociobehavioural research towards more intelligent and inclusive societies.

Dr. Tan has served on the TPC of numerous conferences and reviewer of papers for many key journals and conferences in the area of wireless networks.